Journal of Luminescence 253 (2023) 119474

Contents lists available at ScienceDirect

Journal of Luminescence

journal homepage: www.elsevier.com/locate/jlumin

Full Length Article

Controlled synthesis of GaN square shape nanorods: Their excellent electronic and optical properties for optoelectronics applications

Mudassar Maraj [a], Ghulam Nabi [b,*], Muhammad Tanveer [b], Sajad Hussain [c], Wenwang Wei [a], Muhammad Shakil [d], Muhammad Isa Khan [d], Tahir Iqbal [b], Wajid Ali [b], Wenhong Sun [a,e,**]

[a] Research Center for Optoelectronic Materials and Devices, School of Physical Sciences and Technology, Guangxi University, Nanning, 530004, China
[b] Nanotechnology Lab, Department of Physics, University of Gujrat, Gujrat, 50700, Pakistan
[c] Department of Physics, Division of Science and Technology, University of Education, Lahore, Pakistan
[d] Institute of Physics, The Islamia University of Bahawalpur, Bahawalpur, Pakistan
[e] Guangxi Key Laboratory of Processing for Non-ferrous Metallic and Featured Materials, School of Resources, Environment and Materials, Nanning, 530004, China

ARTICLE INFO

Keywords:
GaN
Semiconductor
Nanowires
Nanorods
I–V characteristics
PL properties

ABSTRACT

High quality square shaped GaN nano-rods are successfully synthesized by a novel method of precursors pre-treatment with aqueous NH_3 via CVD method at 1300 °C. The pre-treatment effect significantly enhanced the conductivities, carrier concentrations and mobilities in GaN nanorods. GaN nanowires have also been synthesized at 1300 °C without treating precursors with aqueous NH_3. Diameter of the nanorods and nanowires are measured in the range of 100-200 nm whereas length is in tenth of microns. Room temperature PL analysis of GaN nanowires displayed a high intensity near-band-edge emission at 370 nm with week blue emission. The GaN square nanorods exhibited the yellow band emission at 565 nm vanishing the weak blue emission along with the near-band-edge emission at 369 nm indicating their potential applications in optoelectronics. The carrier concentrations (N_d) are calculated to be 3.65–5.25 × 10^{16} cm^{-3} and 2.25~5.88 × 10^{18} cm^{-3} for nanowires and nanorods respectively. The electron mobilities (μ) calculated for the GaN nanowires were in the range of 200~300 cm^2/Vs where as for the nanorods were 154~625 cm^2/Vs. The high quality GaN nanorods building blocks with high conductivities, career densities and mobilities will be a tremendous breakthrough in low voltage operating nano-devices.

1. Introduction

The GaN based nanorods have been attracting the scientific community since a decade for their extraordinary features and prospective applications [1–7]. The wurtzite GaN is an exciting semiconductor material which has potential applications in different fields such as lasers [8], LEDs [9], energy solar cells [10], field-effect transistors [11], field emitters [11,12], detectors [9], inverters and bipolar transistors [13] have been fabricated which are crucial and having great interest for broad commercial applications.

Owing the excellent properties of GaN, their size, morphology and electronic properties, one-dimensional nanostructures such as nanorods (NRs), nanowires (NWs) and nanotubes (NTs) made up of GaN have become an essential part of nanoelectronics and nanodevices with extraordinary performance and multipurpose applications such as light emitting diodes, photodetectors, sensors, photocatalysis, probes etc. [14–21]. In the last decade, a great research work has been focused on NWs, NRs and nanotubes made from a wide range of materials but GaN NWs and NRs are particularly promising. Due to this intense recent research interests there are strong motivations for examining the transport properties of single GaN NW and NR for possible applications in different electronic nanodevices.

Recently different synthetic techniques for synthesis of GaN NWs/NRs [8–10,12,13,22–27], nanotubes [28,29], nanoleaves [30], nanoribbons [31], nanorings [32] and nanocolumns [33] have been employed such as molecular beam epitaxy, metal-organic chemical vapor deposition, template growth, chemical vapor deposition, arc-discharge, plasma and laser assisted catalyst and hydride vapor

* Corresponding author.
** Corresponding author. Research Center for Optoelectronic Materials and Devices, School of Physical Sciences and Technology, Guangxi University, Nanning, 530004, China.
E-mail addresses: gnwattoo@uog.edu.pk (G. Nabi), 20180001@gxu.edu.cn (W. Sun).

https://doi.org/10.1016/j.jlumin.2022.119474
Received 7 May 2022; Received in revised form 25 October 2022; Accepted 27 October 2022
Available online 1 November 2022

phase epitaxy [11,13,22–36]. Most commonly used method is chemical-vapor-deposition (CVD) method which is simple and cheaper one. For growing GaN NWs and NRs by CVD method usually gallium metal is used as precursors [23,37,38]. When gallium metal is used as precursor for such growth, there are some issues which have also been mentioned by Li et al. [38].

Having the immense difference between melting point of Ga metal precursor (29.76 °C) and boiling point which is 2204 °C, the Ga metal precursor converted into liquid as the process proceeds. Consequently, it is susceptible that a layer of GaN will be fitted out on the Ga metal spheres. This susceptible GaN layer is liable to stoppage the further reaction of Ga metal with NH_3 gas.

Subsequently, a minor share of Ga metal can react with NH_3 gas which results low yield of GaN product by this method. To avoid this low yield situation and to enhancing the GaN NWs/NRs yield quantity, we have used a novel and facile CVD method. In this novel method, the precursor was pre-treated with aqueous NH_3 (25% w/w) and also high flow rate of NH_3 gas was used. Since the defects and various vacancies such as Ga vacancies and N vacancies have the ability to control the electronics and electrical properties of the nanowires, so the preferred electrical properties can be tuned by varying and adjusting the Ga and N concentration [39]. Pengan Li et al. synthesized GaN nanowires via CVD method and found the NH_3 flow rate is also an important parameter to synthesize various GaN nanostructures. NH_3 gas flow rate has significant effect on the shape and the size of synthesized GaN nanostructures [40]. A higher flow rate of NH_3 gas and treating it with aqueous NH_3 gives a higher N concentration. So in our experiment we have achieved the higher N concentrations by high flow rate of NH_3 gas and also pre-treating with aqueous $NH_{3,}$ which is helpful in increasing the N concentrations and creating the Ga vacancies. These increased level of N concentrations leads to the enhancement of conductivity, charge carrier densities and overall electrical properties of the NRs. So high concentrations of Ga vacancies have been achieved by high flow rate of NH_3 and pre-treating it with aqueous NH_3 which lead to the enhancement of electrical properties. By adjusting the N concentration, the various desired properties (electrical) of the nanowire can be obtained. The NH_3 flow rate ensures the N concentration role in the GaN nanowires. A higher N concentration can be achieved by increasing the flow rate.

Here in this research, the time dependent high quality controlled growth along with high yield of GaN NRs has been made. For comparison purpose, the reaction temperature was made constant at 1300 °C. The controlled growth of GaN NRs/NWs have potential nanotechnological applications. Long NWs/NRs are very crucial for large-scale production of nano-devices. So electrical transport properties of synthesized GaN nanowires and nanorods were also measured which showed that the precursors treated with aqueous NH_3 also has noteworthy enhancement influence on the electronics and optical properties of GaN NRs. The resistivities ($\rho = RA/L$) of the both untreated NWs and pre-treated NRs were calculated which were 0.40–0.85 Ω-cm and 0.0045–0.0070 Ω-cm respectively. The conductivities (σ) of the NWs and NRs were calculated to be 1.17–2.50 $(\text{ohm-cm})^{-1}$ and 140–220 $(\text{ohm-cm})^{-1}$. The significant decrease in resistivity and enhancement in conductivity of pre-treated NRs demonstrates that the conductivity can be increased by treating the precursors with aqueous NH_3. Carrier concentrations calculated for NWs and NRs were (Nd) = 3.65–5.25 × 10^{16} cm^{-3} and 2.25–5.88 × 10^{18} cm^{-3} whereas mobilities were 200-300 cm^2/Vs and 154–625 cm^2/Vs which exhibited that the mobilities and carrier concentrations of the pre-treated GaN NRs are much higher than the untreated GaN NWs. So these results showed that the precursors pre-treated with aqueous NH_3 have significant effect on the conductivity enhancement, charge carrier densities, mobilities and the electrical properties of GaN NRs that have great potential for optoelectronics devices. The significant enhancement in various electrical parameters makes them striking materials for converting into functional low power and electronic devices.

2. Experimental section

Ten grams (10 g) of the gallium metal (AR reagent, the Beijing Chemical Factory) was put into an alumina boat and treated with aqueous ammonia at 100 °C. After the addition of few drops of aqueous ammonia, the gallium metal was agitated with glass rod. GaN powder was obtained from these precursors in horizontal tube (HT) furnace in the flow of NH_3 gas at 1000 °C. For further utilization, GaN powder was analyzed which was pure as shown in XRD graph [Fig. 3(a)]. Then this GaN powder was re-utilized as precursors, untreated and pre-treated with aqueous ammonia at 100 °C five times as mentioned earlier. Silicon wafers (001) having size of 20 × 10 mm^2 were ultrasonically cleaned and used as a substrate for the GaN NWs and NRs growth. Nickel chloride/ethanol solution with concentration 0.02 M was coated on silicon substrates and the GaN NWs/NRs were synthesized using CVD method. Pretreated and untreated GaN powder was loaded in alumina tube and Si substrates were positioned on top of the loaded precursors and the shining side direction was downward facing towards the source material. The vertical distance between loaded precursors and substrates were about 3–4 mm. Then the alumina tube was transferred into HT furnace. After sealing and flushing with NH_3 the flow rate of NH_3 was adjusted at 200 sccm (standard cubic centimeter per minute). A ramp rate of 10 °C/min of the HTF was set to achieve the temperature of 1300 °C. For NWs 1300 °C temperature was maintained for 2 h and for NRs it was maintained for 30–120 min in continuous NH_3 gas flow. At the end, the HTF was naturally cool down till achieving room temperature. A yellowish product was obtained on the substrates for further analysis.

The synthesized products (GaN NWs/NRs) were characterized by various sophisticated characterization techniques such as X-ray powder diffraction (XRD, Philips X'Pert Pro MPD), scanning electron microscopy (SEM, TM-1000, Japan), and energy dispersive X-ray spectrometer (EDS), selected area electron diffraction (SAED) and high-resolution transmission electronic microscope (HRTEM, Tecnai F20). The room temperature photoluminescence (PL) spectra were recorded by using He–Cd laser with a wavelength of 325 nm as the excitation source. Electrical characteristics of GaN nanorods and nanowires were realized by using a Keithley 4200-SCS system.

3. Results and discussion

Fig. 1 depicting the SEM image showing the morphology of as produced NWs and NRs on silicon substrate acquired at various temperatures and conditions. GaN NWs were produced at 1300 °C for 2 h without being treated with aqueous NH_3 as indicated in Fig. 1(a). The diameter of these nanowires was 200–500 nm, and their length was in the tenths of microns. Inset of Fig. 1(a), a high-resolution SEM picture of a single NW was exhibited, revealing that the wire's surface was smooth and its diameter was consistent along its length. Fig. 1 (b) shows GaN NRs pre-treated with aqueous NH_3 and produced at 1300 °C for 30 min. The length of these rods were in range of 5–10 μm and diameter was in the range of about 500–900 nm. Fig. 1 (c) shows the GaN NRs prepared at 1300 °C for 2 h. A lot of random NRs has been distributed the silicon substrate which showed that length of nanorods could be increased by reaction time. The length of these nanorods is about tenths of micrometer and diameter is about 200–400 nm. Most of the nanorods have constant diameter throughout their length. It is praiseworthy to note that mostly NRs have trapezoid or square shape cross sections at their ends as encircled and inset of Fig. 1(d). Main difference in the fabrication process of NRs and NWs was the pretreatment of precursors with the aqueous NH_3 which was the key point in the process for fabricating of square/trapezoid NRs.

The EDS was used to perform the quantitative analysis for the product, as shown in Fig. 2. Fig. 2 (a) illustrates the EDS pattern of untreated GaN NWs on the Si substrate, indicating that the NWs were made up of Ga and N. The usage of a Si substrate resulted in a Si peak in

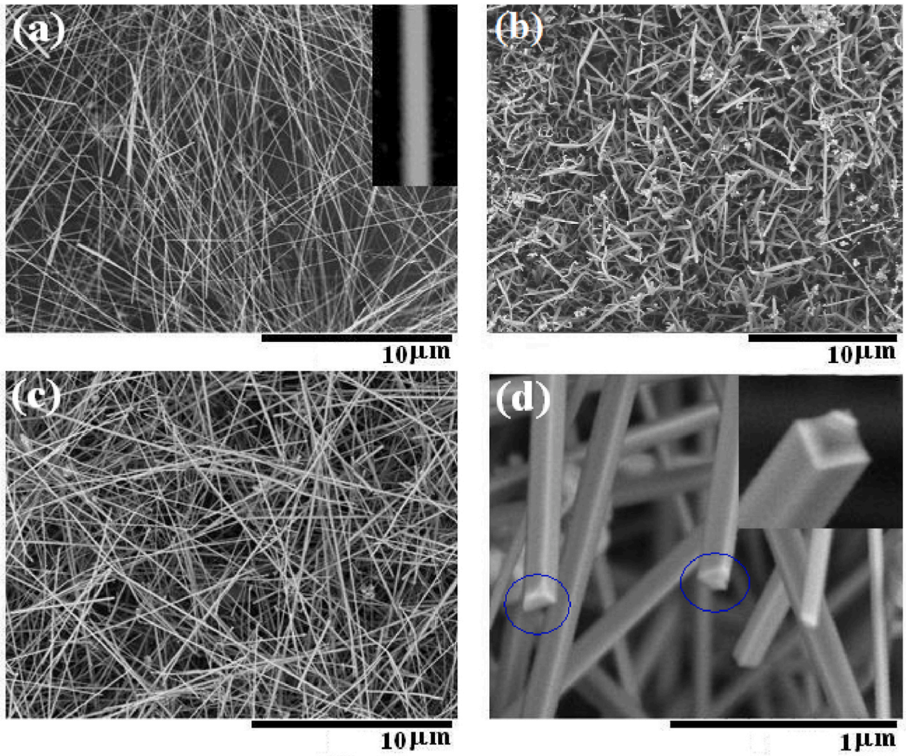

Fig. 1. (a) Showing the SEM image of untreated GaN NWs at 1300 °C (inset is high resolution image), (b) shows the SEM of pre-treated GaN NRs at 1300 °C for 30 min, (c) shows the SEM of the pee-treated GaN NRs at 1300 °C for 2 h, (d) shows the high resolution images of pre-treated GaN NRs prepared at 1300 °C for 2 h showing trapezoid shapes (inset is the square shape of rod).

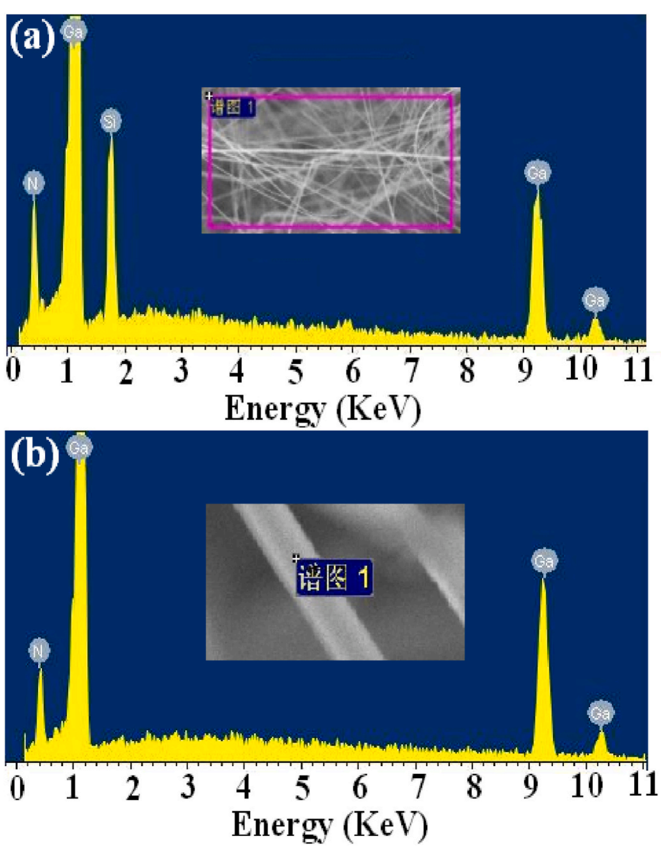

Fig. 2. (a) Shows the EDX pattern of the untreated GaN NWs whereas Fig. 2 (b) shows the EDX pattern of the single pre-treated GaN NR.

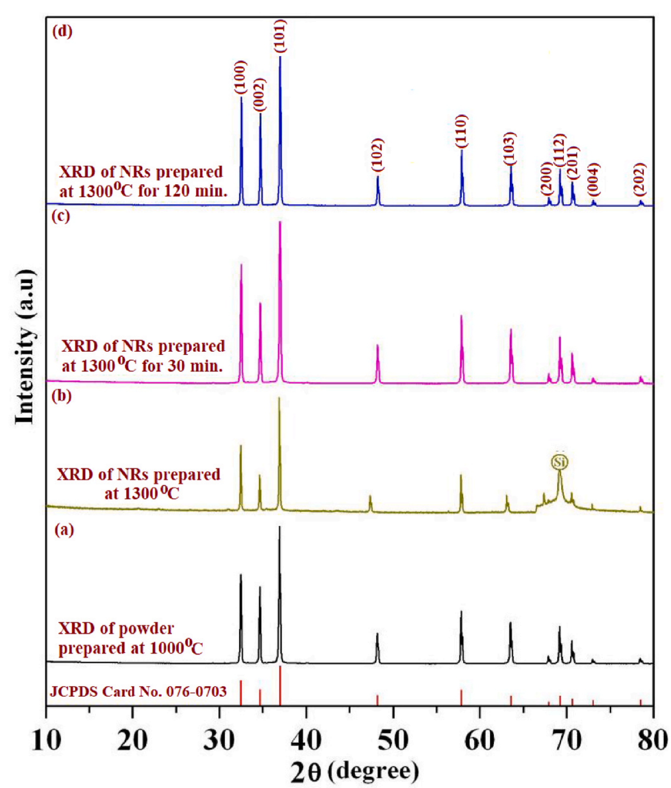

Fig. 3. (a) Shows the XRD pattern of GaN powder prepared at 1000 °C (b) XRD pattern of untreated NWs at 1300 °C (c) XRD pattern of the pre-treated NRs prepared at 1300 °C for 30 min and (d) XRD pattern of the pre-treated GaN NRs prepared at 1300 °C for 120 min.

the EDX. The region with the highest EDS is shown in the inset of Fig. 2 (a). Fig. 2 shows a quantitative examination of GaN NR that has been pre-treated (b). Within the experimental errors, the EDX revealed Ga and N as components of the produced GaN, with an atomic ratio of Ga/N of roughly 1:1. As a result, EDX showed the product's purity. In the EDS pattern of the GaN NRs, no Si peak was observed because EDX pattern was take on single point and also Si substrate was fully covered with the product. Inset of Fig. 2 (b) is the rod whose EDX was performed at single point.

The typical XRD pattern of the as synthesized GaN powder from gallium metal at 1000 °C is shown in Fig. 3 (a). The XRD pattern of the untreated GaN NWs manufactured at 1300 °C is shown in Fig. 3 (b). Because of the usage of silicon substrate and poor yield, a silicon peak developed in the XRD graph of Fig. 3 (b). Fig. 3 (c) shows the XRD of pre-treated GaN NRs deposited on the silicon substrate at 1300 °C for 30 min, whereas Fig. 3 (d) shows the XRD graph of pre-treated GaN NRs grown on the silicon substrate at 1300 °C for 120 min.

No Si peak was observed in these patterns because Si substrate was fully covered with GaN NRs due to high yield of product. The XRD pattern of pre-treated GaN NRs as showed in Fig. 3 (c and d) revealed the phase purity and overall crystal structure of the synthesized GaN NRs. The hexagonal wurtzite GaN with lattice parameters a = 3.188 and c = 5.183 (for GaN NWs a = 3.186 and c = 5.188) may be ascribed to the diffraction peaks in the patterns of GaN NRs, which are in good agreement with JCPDS Card (No.076-0703). In the spectrum, Miller indices of GaN hexagonal structure are also highlighted. The high purity of the GaN wurtzite phase was revealed by the crisp diffraction peaks and strong intensities of the XRD peaks of GaN nanorods diffraction peaks relative to the background signals. The (101) peak had a higher intensity than the (100) and (002) peaks, indicating that the [101] direction was aligned with the NRs axis.

The TEM, HRTEM and SAED characterizations were also done to see the insight of the as-grown untreated GaN NWs and treated GaN NRs as shown in Fig. 4.

In Fig. 4 (a) TEM image of single untreated GaN NW is shown which depict the size of nanowire is 100 nm. In Fig. 4 (b) HRTEM of the untreated NW has been shown which clearly revealing the inter planer distance which is 0.26 nm consistent with XRD pattern. The single crystalline nature of the GaN NWs has been shown by SAED depicted in the inset of Fig. 4(b). The TEM image of the pre-treated GaN NR has been depicted in Fig. 4 (c) and inset is its high resolution image. The HRTEM graph of the single pre-treated GaN NR depicted in Fig. 4 (d). The inter planer distance (d) was 0.25 nm for (100) atomic planes which clearly match with the XRD pattern and is evidence of the purity of GaN NRs. Inset of Fig. 4 (d) SAED pattern has been shown which reveals the crystallinity nature of the product. So both SAED and HRTEM results endorse the effective development of the single-crystalline GaN NWs and NRs having wurtzite nature.

GaN powders treated with aqueous NH_3 have tendency of easy GaN nanorods growth in the presence of Ni catalyst. The growing process for the long GaN nanorods has also been proposed. At the start when temperature of the furnace gradually increases to the range of 800–900 °C which causes NH_3 gas decomposition [41]. With increase of temperature the catalyst nickel chloride also decays to convert into nanometer-sized nickel particles. These nickel nanoparticles plays an effective role in synthesis of GaN nanorods [42]. At the same time, the GaN powder treated with aqueous NH_3 located at the center of the furnace vaporized. These vapor-phases GaN absorbed on the energetically favorable sites of Ni particles. As long as absorbed GaN nucleoids reaches saturation point, the nanorods and nanowires start to nucleate and growing in good way. With consistent and steady immersion GaN nucleoid containing vapor-phase GaN particles, GaN NRs/NWs were developed on Si (001) substrate having very high density adopting via vapor-liquid-solid (VLS) mechanism [38]. It was also confirmed with several experiments that

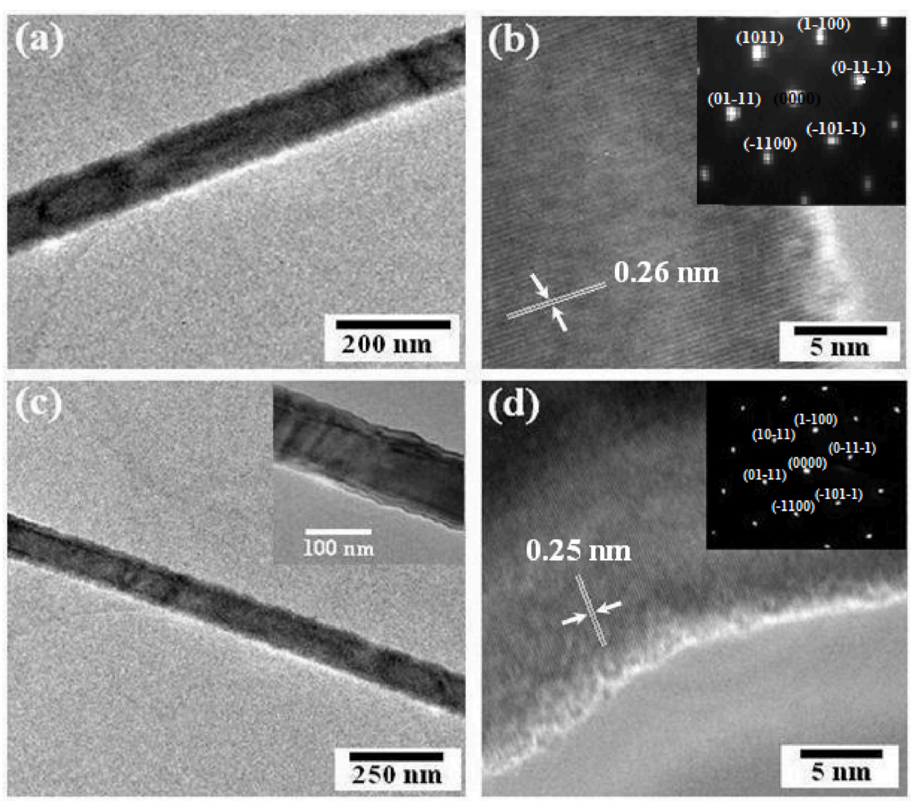

Fig. 4. (a) Shows the untreated GaN NW TEM prepared at 1200 °C, (b) shows the HRTEM of NW (inset is the SAED) (c) depicting the TEM image of the pre-treated GaN NR prepared at 1300 °C for 120 min (inset is high resolution image), (d) shows the HRTEM of the single GaN NR prepared at 1300 °C for 120 min (inset is the SAED pattern).

without treating the precursors only nanowires are produced but when GaN powder was treated with aqueous NH_3 then at 1300 °C it surly synthesis the GaN nanorods. It is worth noting that this work is highly reproducible and these rods have excellent electronic properties which will be discussed later in detail.

3.1. Photoluminescence

Optical characterizations of single GaN NW and NR were studied by PL spectrum at room temperature. The 325 nm excitation wavelength was used in PL process and PL of untreated single GaN NWs has been portrayed in Fig. 5 (a). A strong emission peak at 370 nm (3.35 eV) has been shown which is credited to near band edge emission [38]. Two smaller shoulder peaks at 446 nm and 462 nm in blue luminescence region are also observed caused by nitrogen vacancies.

Photoluminescence measurements of single pre-treated GaN NR have been depicted in Fig. 5 (b). Comparatively a narrow near band edge emission peak at 369 nm (3.36 eV) is obtained attributed to the band-edge emission [38,43]. Single narrow PL emission peak of NR indicated that the GaN NRs pre-treated grown GaN have virtuous optical quality appropriate for optoelectronic devices [44].

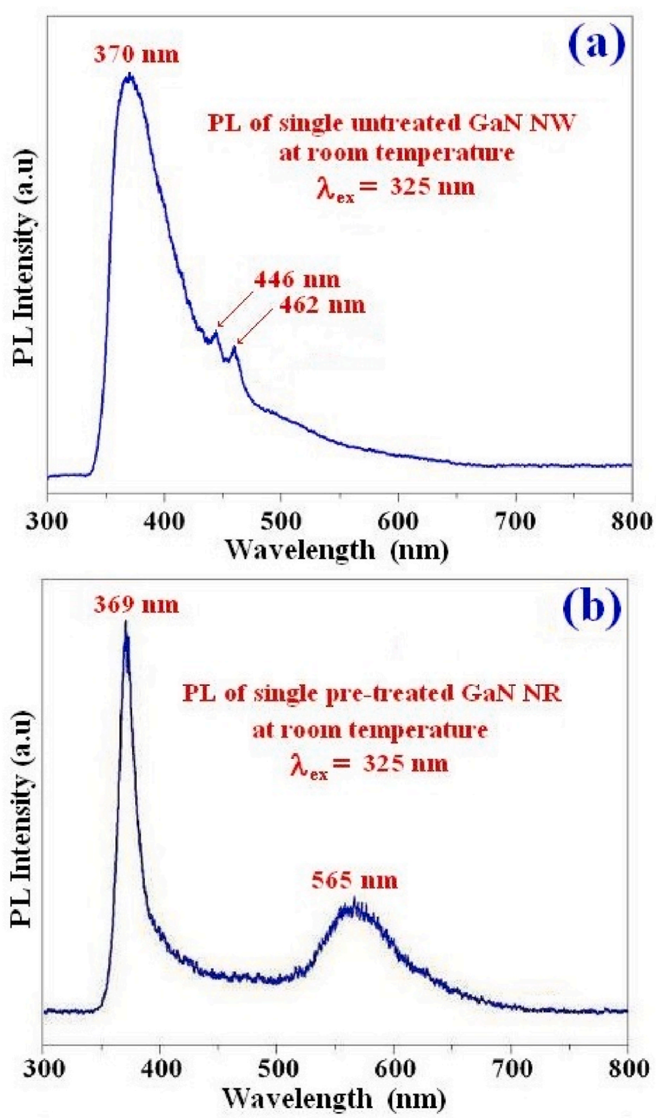

Fig. 5. (a) The PL emission spectrum of single untreated GaN NW measured at room temperature (b) depicting PL emission spectrum of single pre-treated GaN NR prepared at 1300 °C for 120 min measured at room temperature.

A broad peak at 565 nm (2.19eV) having comparatively low intensity is also observed on the square shaped GaN NRs. The PL emission peak at 565 nm in yellow luminescence region, ascribed to the Ga vacancies and defect related emissions [44]. Such kind of yellow emission peak was also observed by Godhuli Sinha et al. has also related observations in yellow luminese region [45] which are most probably related to deep levels or defect levels. So, this yellow luminescence is due to the Ga vacancies which are created by pre-treatment effect of aqueous NH_3 and are also responsible for good electrical characteristics.

The full width half maximum of the nanowires/nanorods have been calculated as 46.95 and 20.25. The FWHM provides the information about the homogeneous and inhomogeneous broadening of the natural linewidth of the transition, which can be related to crystallinity disorder. In the lines shape, a Lorentzian is an ideal line shape, and deviation to a Gaussian indicated disorder in the PL graph. A PL spectrum may also have phonon side bands. In addition, the inhomogeneity might be caused by band gap fluctuations, which can be due to chemical fluctuations or electrostatic potential variations. Latter one can be also related to the degree of compensation, i.e. the ratio of donors to acceptors. If you have locally a high density of donors or acceptors, which cannot be screened, then you get band gap fluctuations leading to a broadening of your PL peak. Hence, the FWHM of a peak also reveals insights of the material which is under observation. For the comparison purpose, comparison of PL emission Peaks of various GaN nanostructures have been depicted in Table 1.

4. Characteristics

Electronic properties of GaN are the core of their applications in nano-devices [55,56]. In this study, the Electronic transport characteristics were measured using a 4200-SCS Keithley apparatus and KZ100, Keithley-Zyvex, nano-probing system. Measurements were performed under direct SEM observation. In this research paper electrical properties of long untreated NWs and pre-treated NRs have been measured, in which the electronic transport working in the diffusive regime. Therefore, Ohmic law is effective to elucidate the conduction of carriers in the un-depleted regimes of the NWs/NRs. For the semiconducting I–V characteristics measurements of NW and NR, two electrodes of metals were made into contact. Two Schottky barriers designed at the contact places i.e. between NW/NR and the metal electrodes. It's well established that the contacts between metal electrodes and the NW/NR have been a significant subject in explaining the I–V characteristics of devices which is affected significantly by its contacts with electrodes [57]. For preparing the samples one single GaN NW/NR was transported to the Au

Table 1
PL emission peak positions of various GaN nanostructures grown by different methods.

Sr #	Synthesis method	Morphology obtained	Emission peak	Ref
1.	Chemical vapor deposition (CVD) method	Hexagonal micro-bricks	369 nm 556 nm	[46]
2.	Pulsed laser deposition	Cauliflower-like	541 nm	[47]
3.	Low-pressure chemical vapor deposition (LPCVD)	Hexagonal rod	363 nm	[48]
4.	Infrared close space vapor transport (CSVT-IR)	Polycrystalline	521 nm	[49]
5.	MOCVD	Porous GaN films	357 nm	[50]
6.	Hydride vapor phase epitaxy (HVPE)	Nanowires	400 nm	[51]
7.	Pulsed laser deposition	Spherical clusters	590 nm	[52]
8.	Chemical vapor transport method	GaN nanowires	563 nm	[53]
9.	Molecular beam epitaxy	GaN QDs	332 nm	[54]
10.	Chemical vapor deposition (CVD) method	Nanowires	370 nm 462 nm	This work
11	Chemical vapor deposition (CVD) method	Nanorods	369 nm 565 nm	This work

grid which is available commercially in the market. For achieving a decent physical contact at two ends silver paint was employed. Later, a high temperature was delivered by Joule heating phenomenon for welding purpose. In this way GaN NW/NR have been welded with two electrodes. In this way a minimum contact resistance (Rc) electrical contact was realized as in Fig. 6. Fig. 6 (a) is depicting I–V characteristics of single untreated GaN NW and in the inset, right side of the bottom is the Ln I vs bias V. In Fig. 6 (b) the I–V characteristics of single pre-treated GaN NR have been shown. Whereas inset of top left is actual rod diagram whose I–V characteristics were measured. At the right side bottom is the logarithmic current (Ln I) vs bias V.

Normally, depending upon the contacts and Schottky barriers, distinct *I–V* characteristics have been observed which include almost linear [58–60], almost symmetric [57,61], asymmetric [62–64] and almost rectifying [65,66]. Measurements of untreated GaN NWs and pre-treated GaN NRs showed almost symmetric behaviors as publicized in Fig. 6 (a, b). Semiconducting *I–V* characteristics of NWs/NRs depend on various intrinsic parameters including Schottky barrier height, resistivity, carrier mobility, contact geometry and contact area. Based on previous studies of bulk materials, n-type and almost symmetric behavior in un-doped GaN is attributed to the nitrogen, gallium or oxygen vacancies [11,45]. But in our case oxygen impurities were not observed as shown in EDX pattern so we believe that such kind of behavior is only due to the nitrogen vacancies or gallium vacancies which regulates the I–V characteristics of the GaN NWs/NRs.

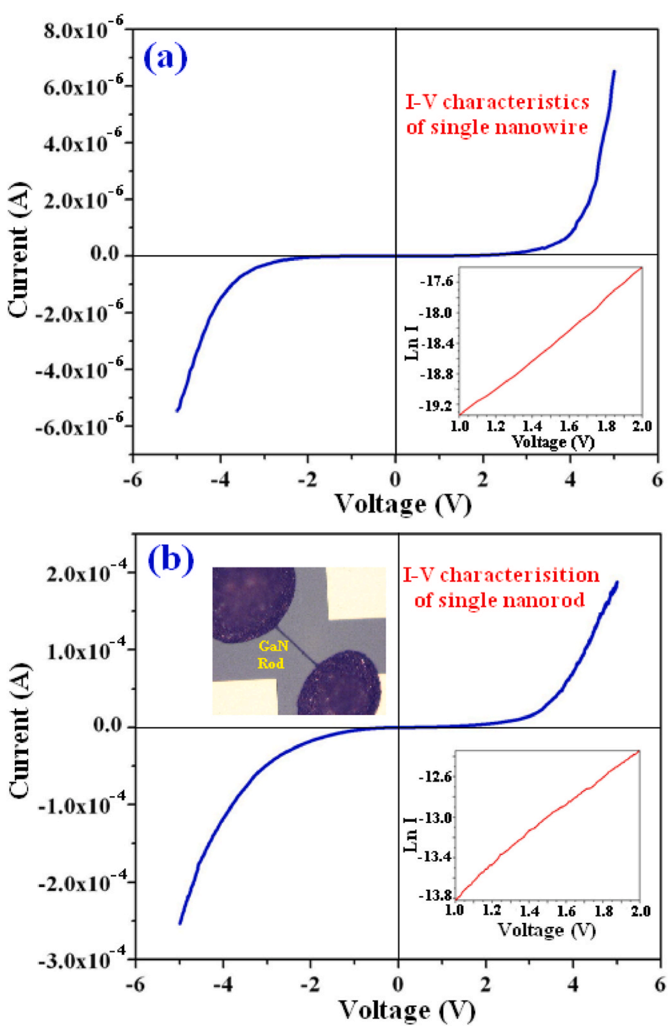

Fig. 6. (a) Depicting GaN I–V curve of single untreated NW. Inset, right side of the bottom is the Ln I vs bias V. (b) Shows the GaN I–V curve of single pre-treated NR whereas inset of top left is actual rod diagram whose I–V characteristics were measured. At the right side bottom is the logarithmic current (Ln I) vs bias V.

Since, here GaN NW and NR contacts have been made of two electrodes so Metal Semiconductor Metal (M-S-M) model can be applied as depicted in Fig. 7. It's a well know reality that a Schottky barrier established at the metal-semiconductor interface have important role in such M-S-M electrical transport structure [67].

M-S-M based I–V characteristics model plays the crucial part only when the NW/NR radius is larger enough as compared to de Broglie wavelength. Majority of semiconducting NWs/NRs synthesized have larger size than their corresponding de Broglie wavelengths which is about 2–20 nm. Hence, this M-S-M model can be employed to analyze I–V characteristics of these nanostructures. To make the calculations simple and convenient the Ohmic contact were also considered as Schottky barrier. So, M-S-M model may be structured and modeled as consisting of two Schottky barriers which are in back to back series connection in semiconducting NW/NRs with resistance *R* as displayed in Fig. 7. In this way, *I–V* characteristic curves are explained by means of contacts in two metal electrodes and the NW/NR instead of nanowire itself. The M-S-M schematic diagram and its corresponding circuit diagram is depicted in Fig. 7. Multiple *I–V* curves of various synthesized NWs/NRs were measured to ensure reproducibility and semiconducting nature of the NWs/NRs.

The reverse-biased Schottky barrier voltage, the forward-biased Schottky barrier voltage and the NW/NR voltage are symbolized as V_1, V_2 and V_{NR}, respectively as publicized in Fig. 7. The total voltage V is given as

$$V = V_1 + V_{NR} + V_2 \tag{1}$$

The most effectively used thermionic emission theory is used to explain the planner Schottky junctions for M-S-M modeling in modern microelectronic devices [67]. Although this theory fails in some cases, such as in single electron transistors case [68] and some carbon based nanoelectronic devices [69] due to significant electron tunneling, but in current case it works well to examine the semiconducting I–V characteristics. As per thermionic emission theory current density (J) for Schottky junction for forward biased can be given as

$$J(V, \Phi_1) = A * T^2 \exp\left(-\frac{\Phi_1}{kT}\right)\exp\left(\frac{qV}{nkT}\right) \times \left\{1 - \exp\left(-\frac{qV}{kT}\right)\right\} \tag{2}$$

Where $A^* = 4\pi m^* qk^2/h^3$ is the Richardson constant of the semiconductor. Unlikely, this thermionic emission theory misjudges the reverse current. However, for symmetric *I–V* characteristics in current case, the situation is entirely different. In this model, the reverse current and forward current are practically in same range indicating the reverse-biased barrier current tunneling explainable on the basis of thermionic field emission theory [67]. The current transport here in this measurements for the forward-biased Schottky barrier still follows the thermionic-emission theory. The thermionic emission theory only lacks in the tunneling current as it has significant impact on the reverse bias measurements in low dimension nano-systems [69] which is required to

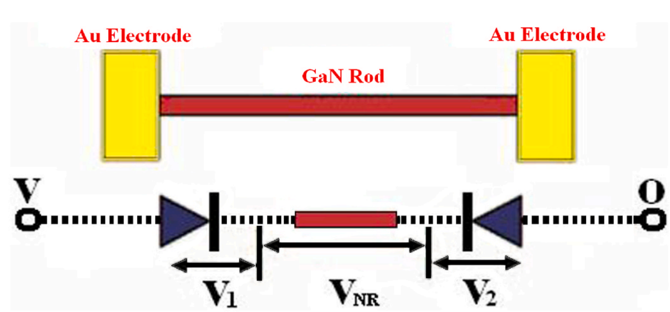

Fig. 7. Shows the schematic diagram along with its corresponding circuit (dotted line) for M-S-M model.

be included in a more general thermionic field emission theory. So, the reverse tunneling current density through the left Schottky barrier as per thermionic field emission theory is expressed as [67].

$$J_1(V_1,\Phi_1) = -J(V_1,\Phi_1)\times \exp\left\{V_1\left(\frac{q}{kT}-\frac{1}{E_0}\right)\right\} \tag{3}$$

Where J varies slowly with applied bias and is given as

$$J = \frac{A*T(\pi q E_{00})^{1/2}}{k}\exp\left(\frac{\Phi_1}{qE_0}\right)\times\left\{q(v_1-\zeta)+\frac{\Phi_1}{\cosh^2(qE_{00}/kT)}\right\}^{1/2} \tag{4}$$

Where ζ represents the distance between the bottom of the conduction band and Fermi energy and Φ_1 represents the active Schottky barrier. From the Model M-S-M as in Fig. 7 we have

$$E_0 = E_{00}\coth\left(\frac{qE_{00}}{kT}\right) \tag{5}$$

with

$$E_{00} = \frac{\hbar}{2}\left(\frac{N_d}{m_n^*\varepsilon_s\varepsilon_0}\right)^{1/2} \tag{6}$$

Whereas h and $\hbar$ are the Planck constants, N_d = donor density at the semiconductor-metal interface, ε_s is dielectric coefficient of the semiconducting nanostructure and ε_0 represents the free space dielectric coefficient.

Another significant tunneling theory parameter is E_{oo} which deals with the Schottky barrier diffusion potential in the transmission probability for the electrons.

As expressed by the thermionic field emission theory, the forward current density through the right Schottky barrier is expressed as [56].

$$J_2(V_2,\Phi_2) = A*T^2\exp\left(\frac{qV_2}{nkT}\right)\exp\left(-\frac{q\Phi_2}{kT}\right)\times\left\{1-\exp\left(-\frac{qV_2}{kT}\right)\right\} \tag{7}$$

Where Φ_2 represents the active Schottky barrier potential height. The current should be the equivalent flowing through the forward-biased Schottky barrier and the reverse-biased Schottky barrier, the NW/NR which is denoted as:

$$I = S_1J_1(V_1,\Phi_1) = \frac{V_{NR}}{R} = S_2J_2(V_2,\Phi_2) \tag{8}$$

Here contacts area of reverse-biased and forward-biased Schottky barrier is represented by the symbols S_1 and S_2 respectively and are assumed to be equal to the cross sectional area of the NW/NR.

Putting the value of J_1 from equation (3) into equation (8) can be obtained

$$I = S_1\left[-J(V_1,\Phi_1)\times\exp\left\{V_1\left(\frac{q}{kT}-\frac{1}{E_0}\right)\right\}\right] \tag{9}$$

So

$$\ln I = \ln S_1 - \ln J(V_1,\Phi_1) + V_1\left(\frac{q}{kT}-\frac{1}{E_0}\right) \tag{10}$$

Since J is insensitive to applied bias V_1, so the plot of lnI verses V_1 is linear as shown in bottom right of Fig. 6 (a, b) and the slope is $m = \frac{q}{kt} - \frac{1}{E_0}$

As we can see clearly form Fig. 6 (a, b) that a major current improvement in the pre-treated GaN NRs has been detected as associated with the untreated GaN NW. At a voltage slightly higher than 4 V, at the stage of varying current linearly along with voltage, the relation, $R \approx dV/dI$ can be used after I–V curves differentiation for calculating the resistance (R) of the NWs/NRs. Thus the resistance linked with GaN NWs/NRs can be estimated from the corresponding slope of the LnI–V as shown in the right below of Fig. 6 (a, b). Using this practical approach and length and diameter from TEM, the resistivity (ρ) = (RA/L) of untreated NWs and pre-treated NRs was calculated to be 0.40–0.85 Ω-cm and 0.0045–0.0070 Ω-cm respectively. The substantial resistivity decrease reveals that the improvement (resistivity decrease) is possible by aqueous NH_3 treatment to the precursors. The conductivity (σ) of the NWs and NRs was calculated by using σ = L/RA. Conductivity calculated for the NWs was 1.17–2.5 $(\text{ohm-cm})^{-1}$ and for NRs is 140–220 $(\text{ohm-cm})^{-1}$. Conductivity results also showed that NRs have better conductivity as compared to NWs. These results exhibit that the conductivity has been enhanced due to the treating precursors with the aqueous NH_3.

For the purpose to regain quantitatively various central factors of the NWs and NRs, M-S-M model was validated. Considering MSM model, the mainstream voltage drop is ascribed due to reverse-biased Schottky barrier (medium biased), whereas most of voltage drop is attributed to the NW/NR itself, which is at high bias as exposed in Fig. 6 (a,b). That's why, the preliminary value of the substantial tunneling parameter E_o has been estimated with the help of the slope in ln I–V as shown in the inset of the right bottom of Fig. 6 (a,b). Using this approach we have obtained E_o = 0.42354 meV and E_o = 0.02675 meV for NWs and NRs respectively whereas carrier concentrations (N_d) = 3.65–5.25 × 10^{16} cm^{-3} and 2.25–5.88 × 10^{18} cm^{-3} were calculated for untreated GaN NWs and pre-treated NRs. Both of these values are consistent with that of GaN material and show the significant enhancement due to pre-treating with aqueous NH_3. The increase in the conductivity of the GaN NRs is the result of the increase in the mobility, which can be measured by equation below

$$Mobility(\mu) = \frac{1}{N_d q\rho} = \frac{\sigma}{N_d q} \tag{11}$$

Mobility measured for GaN NWs were 200–300 cm^2/Vs and for GaN NRs were 154–625 cm^2/Vs which showed that the mobility of the pre-treated GaN NRs is much higher than the untreated GaN NWs. So the present results ascertain the noteworthy effect on the improvement of conductivity by pre-treating the precursors with aqueous NH_3. The improvement in charge carrier densities and electrical properties of the NRs have great potential for optoelectronics devices.

Since various vacancies have the ability to control the electrical properties, so the desired electrical properties can also be tuned by regulating the N and Ga concentration. The higher flow rate of NH_3 gas and treating it with aqueous NH_3 gives a higher N concentration creating Ga vacancies which are also observed in the PL emission depicted in Fig. 5 (b). So in our experiment we have achieved the higher nitrogen concentrations by high flow rate of NH_3 gas and also pre-treating with aqueous NH_3, which is helpful in increasing the N concentrations. These increased level of N concentrations (Ga vacancies) leads to the enhancement of conductivity, charge carrier densities the electrical properties of the NRs.

A comparison of transport results and other different parameters

Table 2
Shows comparison of transport results for single GaN Nanowires/Nanorods.

S#	Shape	Length (μm)	Diameter (nm)	μ (cm^2/Vs)	N_d (cm^{-3})	Ref
1	Conical wires	15	100	30	2 × 10^{17}	[27]
2	Triangular cross section	5	5–100	65	4 × 10^{18}	[15]
3	Quasi circular	4	17.6	150–650	10^{18}–10^{19}	[9]
4	Quasi circular	0.33	15	2.15	–	[70]
5	nanowires	10	67 ± 20	–	≥ 5 × 10^{18}	[71]
6	nanowires	2	15	83		[22]
7	Nanocolumns	0.3–1	20–80	–	5 × 10^{17}	[38]
8	Wires			15	5 × 10^{17}	[72]
9	Circular nanowires	10–20	100–150	200–300	≥3.65 × 10^{16}	**Our result**
10	Square/ trapezoid Nanordos	10–20	150–200	154–625	≥2.25 × 10^{18}	**Our result**

such as length and diameter of GaN materials has been given below in Table 2.

On comparing these values, it can be seen that our results are consistent with Gallium Nitride (GaN) materials. The electrical properties, carrier concentrations and the mobilities of pre-treated GaN nanorods are much better than already reported values. The high carrier concentrations and mobilities measured in the pre-treated GaN NRs make them striking building blocks for various useful electronic devices. This significant increase in the mobility and conductivity could be a building block for using it in low power devices and optoelectronics devices. GaN square/trapezoid nanorods also have low resistance and huge current flow. So the pre-treated GaN NRs have much better conductivity than other GaN wires and other reported values which is a tremendous breakthrough in low voltage device fabrication.

5. Conclusions

A novel method for synthesizing pure and single crystal square/trapezoid shape GaN nanorods by pre-treating the precursors with aqueous NH_3 has been described due to which significant enhancement in conductivity was observed at low voltage. Electronic transport properties measurements showed that the N_d for untreated NWs was 3.65–5.25 $\times 10^{16}$ cm^{-3} and for pre-treated NRs was 2.25–5.88 $\times 10^{18}$ cm^{-3}. Electron mobilities determined for the GaN NWs were in the range of 200–300 cm^2/Vs where as for the NRs were 154–625 cm^2/Vs. The mobilities of the pre-treated GaN NRs are much better than the untreated GaN NWs and also better than already reported values of GaN materials. These high quality GaN nanorods building blocks with better mobilities will be a tremendous breakthrough in low voltage and nanoscale electronic device fabrication. The reproducible behavior exhibited by these nanorods also suggests significant promise for opening up many exciting opportunities in nano-scale science and technology in practical ways. From PL measurements it was concluded that as synthesized GaN NRs have strong near band edge emission at 369 nm (3.36 eV) with yellow emission which is suitable for potential application in light-emitting devices.

Authors statement

Mudassar Maraj: Methodology, Investigation, Writing, **Ghulam Nabi**: Conceptualization, Supervision, Methodology, Writing, **Muhammad Tanveer**: Resources, Review & Editing, **Sajad Hussain**: Writing, Formal analysis, Data curation, **Wenwang Wei**: Review & Editing, Formal analysis, **Muhammad Shakil**: Writing, Formal analysis, Data curation, **Muhammad Isa Khan**: Writing, Formal analysis, Data curation, **Tahir Iqbal**: Revision, Formal analysis, **Wajid Ali**: Review and editing, Data curation, **Wenhong Sun**: Conceptualization, Supervision, Review & Editing.

Declaration of competing interest

The authors declare that they have no known competing financial interests or personal relationships that could have appeared to influence the work reported in this paper.

Data availability

No data was used for the research described in the article.

Acknowledgements

The authors acknowledge the supported in part by the funding (Nos. T31200992001 and T3120097921) for the Bagui Talent of Guangxi province, Talent Model Base (No. 19110157 CE), Disinfection Robot Based on High Power AlGaN-based UVLEDs (No. BB31200014), Guangxi Science and Technology Program (No. 19245132 CE), Guangxi Science and Technology Base and Talent Special Project (No. 2023893 CE). Guangxi Science and Technology Base and Talented Special project (No. 20238088 CE). The authors also acknowledge the support of Prof. CB Cao (BIT) Beijing, China for lab facilities.

References

[1] S. Zhang, et al., Fabrication and repair of GaN nanorods by plasma etching with self-assembled nickel nanomasks, Eur. Phys. J. Appl. Phys. 93 (3) (2021).
[2] M. Reddeppa, et al., GaN nanorods on V-groove textured Si (111): significant light trapping for photoelectrocatalytic water splitting, Appl. Phys. Lett. 119 (2) (2021), 023901.
[3] C. Ramesh, et al., Controlled growth of GaN nanorods directly on flexible Mo metal foil by laser molecular beam epitaxy, Mater. Sci. Semicond. Process. 111 (2020), 104988.
[4] A.M. Nahhas, Review of GaN nanowires based sensors, Am. J. Nanomater. 8 (1) (2020) 32–47.
[5] C. Ramesh, et al., Structural and optical properties of low temperature grown single crystalline GaN nanorods on flexible tungsten foil using laser molecular beam epitaxy, Mater. Res. Express 6 (8) (2019), 085919.
[6] F. Chen, X. Ji, S.P. Lau, Recent progress in group III-nitride nanostructures: from materials to applications, Mater. Sci. Eng. R Rep. 142 (2020), 100578.
[7] S. Chattopadhyay, et al., One-dimensional group III-nitrides: growth, properties, and applications in nanosensing and nano-optoelectronics, Crit. Rev. Solid State Mater. Sci. 34 (3–4) (2009) 224–279.
[8] F. Qian, et al., Multi-quantum-well nanowire heterostructures for wavelength-controlled lasers, Nat. Mater. 7 (9) (2008) 701–706.
[9] Z. Zhong, et al., Synthesis of p-type gallium nitride nanowires for electronic and photonic nanodevices, Nano Lett. 3 (3) (2003) 343–346.
[10] Y. Tang, et al., Vertically aligned p-type single-crystalline GaN nanorod arrays on n-type Si for heterojunction photovoltaic cells, Nano Lett. 8 (12) (2008) 4191–4195.
[11] Y. Huang, et al., Gallium nitride nanowire nanodevices, Nano Lett. 2 (2) (2002) 101–104.
[12] E. Stern, et al., Electrical characterization of single GaN nanowires, Nanotechnology 16 (12) (2005) 2941.
[13] V. Derycke, et al., Carbon nanotube inter-and intramolecular logic gates, Nano Lett. 1 (9) (2001) 453–456.
[14] D. Verheij, et al., Radiation sensors based on GaN microwires, J. Phys. Appl. Phys. 51 (17) (2018), 175105.
[15] M. Spies, et al., Effect of the nanowire diameter on the linearity of the response of GaN-based heterostructured nanowire photodetectors, Nanotechnology 29 (25) (2018), 255204.
[16] S. Cuesta, et al., Effect of bias on the response of GaN axial p–n junction single-nanowire photodetectors, Nano Lett. 19 (8) (2019) 5506–5514.
[17] N. Guan, et al., Colour optimization of phosphor-converted flexible nitride nanowire white light emitting diodes, J. Phys.: Photon. 1 (3) (2019), 035003.
[18] M.A. Johar, et al., Universal and scalable route to fabricate GaN nanowire-based LED on amorphous substrate by MOCVD, Appl. Mater. Today 19 (2020), 100541.
[19] M. Liu, et al., GaN nanowires as a reusable photoredox catalyst for radical coupling of carbonyl under blacklight irradiation, Chem. Sci. 11 (30) (2020) 7864–7870.
[20] S. Yngman, et al., GaN nanowires as probes for high resolution atomic force and scanning tunneling microscopy, Rev. Sci. Instrum. 90 (10) (2019), 103703.
[21] S. Mariana, et al., Vertical GaN nanowires and nanoscale light-emitting-diode arrays for lighting and sensing applications, ACS Appl. Nano Mater. 2 (7) (2019) 4133–4142.
[22] W. Han, et al., Synthesis of gallium nitride nanorods through a carbon nanotube-confined reaction, Science 277 (5330) (1997) 1287–1289.
[23] X. Chen, et al., Straight and smooth GaN nanowires, Adv. Mater. 12 (19) (2000) 1432–1434.
[24] H.M. Kim, et al., Growth of GaN nanorods by a hydride vapor phase epitaxy method, Adv. Mater. 14 (13–14) (2002) 991–993.
[25] T. Kuykendall, et al., Metalorganic chemical vapor deposition route to GaN nanowires with triangular cross sections, Nano Lett. 3 (8) (2003) 1063–1066.
[26] R. Calarco, et al., Size-dependent photoconductivity in MBE-grown GaN−Nanowires, Nano Lett. 5 (5) (2005) 981–984.
[27] C.-Y. Chang, et al., Electrical transport properties of single GaN and InN nanowires, J. Electron. Mater. 35 (4) (2006) 738–743.
[28] J. Li, et al., Synthesis of GaN nanotubes, J. Mater. Sci. Lett. 20 (21) (2001) 1987–1988.
[29] J. Goldberger, et al., Single-crystal gallium nitride nanotubes, Nature 422 (6932) (2003) 599–602.
[30] J. Li, et al., Physical and electrical properties of chemical vapor grown GaN nano/microstructures, Inorg. Chem. 47 (22) (2008) 10325–10329.
[31] J. Li, et al., Morphologies of GaN one-dimensional materials, Appl. Phys. A 71 (5) (2000) 587–588.
[32] J. Li, et al., Gallium nitride nano-ribbon rings, J. Phys. Condens. Matter 13 (14) (2001) L285.
[33] M. Niebelschütz, et al., Electrical performance of gallium nitride nanocolumns, Phys. E Low-dimens. Syst. Nanostruct. 37 (1–2) (2007) 200–203.
[34] G. Steinhoff, et al., AlxGa1–xN—a new material system for biosensors, Adv. Funct. Mater. 13 (11) (2003) 841–846.
[35] Y. Huang, et al., Logic gates and computation from assembled nanowire building blocks, Science 294 (5545) (2001) 1313–1317.

[36] Z. Fang, et al., Axial p–n junction and space charge limited current in single GaN nanowire, Nanotechnology 29 (1) (2017), 01LT01.
[37] J. Li, et al., Conversion between hexagonal GaN and β-Ga2O3 nanowires and their electrical transport properties, Nano Lett. 6 (2) (2006) 148–152.
[38] J. Li, Z. Yang, H. Li, Electrical and optical performance of sublimation-grown long GaN nanowires, J. Phys. Chem. C 114 (41) (2010) 17263–17266.
[39] J.-R. Kim, et al., Temperature-dependent single-electron tunneling effect in lightly and heavily doped GaN nanowires, Phys. Rev. B 69 (23) (2004), 233303.
[40] P. Li, Y. Liu, X. Meng, GaN nanowires and nanotubes growth by chemical vapor deposition method at different NH3 flow rate, Rev. Mexic. Fisica 62 (3) (2016) 219–222.
[41] F. Zong, et al., Structural characterization of Zn3N2 nanowires prepared by nitridation technique, Mater. Lett. 59 (21) (2005) 2643–2646.
[42] C.-C. Chen, et al., Catalytic growth and characterization of gallium nitride nanowires, J. Am. Chem. Soc. 123 (12) (2001) 2791–2798.
[43] X. Xie, et al., Zn-doped gallium nitride nanotubes with zigzag morphology, J. Phys. Chem. C 113 (33) (2009) 14633–14637.
[44] Z. Feng, et al., Influence of Fe-doping on GaN grown on sapphire substrates by MOCVD, J. Cryst. Growth 309 (1) (2007) 8–11.
[45] G. Sinha, D. Ganguli, S. Chaudhuri, Ga2O3 and GaN nanocrystalline film: reverse micelle assisted solvothermal synthesis and characterization, J. Colloid Interface Sci. 319 (1) (2008) 123–129.
[46] G. Nabi, et al., Photoluminescence and hydrogen storage properties of gallium nitride hexagonal micro-bricks, Mater. Lett. 79 (2012) 212–215.
[47] Contreras-Puente, L.A.M.-A.R.A.-H.S.-H.A.H.-H.d.l.Á.H.-P.M.-A.M.-P., Structural and optical properties of GaN thin films grown on Si (111) by pulsed laser deposition, Mater. Res. 22 (2019).
[48] S. Fischer, et al., On the nature of the 3.41eV luminescence in hexagonal GaN, J. Cryst. Growth 189–190 (1998) 556–560.
[49] G. Santana, et al., Photoluminescence study of gallium nitride thin films obtained by infrared close space vapor transport, Materials 6 (2013) 1050–1060, https://doi.org/10.3390/ma6031050.
[50] T.H. Ngo, et al., Enhanced excitonic emission efficiency in porous GaN, Sci. Rep. 8 (1) (2018), 15767.
[51] A.T. Nguyen, et al., Stable and reversible photoluminescence from GaN nanowires in solution tuning by ionic concentration, Nanoscale Res. Lett. 16 (1) (2021) 45.
[52] H.D. Jabbar, M.A. Fakhri, M.J. AbdulRazzaq, Synthesis Gallium Nitride on Porous Silicon Nano-Structure for Optoelectronics Devices, Silicon, 2022.
[53] V. Suresh Kumar, J. Kumar, Growth, surface morphology and optical properties of gallium nitride nanowires, Adv. Mater. Res. (2007) 31.
[54] C. Rothfuchs, et al., Photoluminescence of gallium ion irradiated hexagonal and cubic GaN quantum dots, Nucl. Instrum. Methods Phys. Res. Sect. B Beam Interact. Mater. Atoms 383 (2016) 1–5.
[55] A. Mozharov, et al., Study of electrical properties of single GaN nanowires grown by molecular beam epitaxy, in: Journal of Physics: Conference Series, IOP Publishing, 2016.
[56] A.M. Mozharov, et al., Study of electrical properties of single GaN nanowires grown by molecular beam epitaxy, J. Phys. Conf. 741 (2016), 012002.
[57] Z. Zhang, et al., Current-voltage characteristics and parameter retrieval of semiconducting nanowires, Appl. Phys. Lett. 88 (7) (2006), 073102.
[58] Y.-H. Lee, et al., Co-doped TiO 2 nanowire electric field-effect transistors fabricated by suspended molecular template method, Appl. Phys. Lett. 86 (3) (2005), 033110.
[59] D. Zhang, et al., Electronic transport studies of single-crystalline In2O3 nanowires, Appl. Phys. Lett. 82 (1) (2002) 112–114.
[60] Y. Cui, et al., Doping and electrical transport in silicon nanowires, J. Phys. Chem. B 104 (22) (2000) 5213–5216.
[61] Y. Liu, et al., Quantitative fitting of nonlinear current–voltage curves and parameter retrieval of semiconducting nanowire, nanotube and nanoribbon devices, J. Nanosci. Nanotechnol. 8 (1) (2008) 252–258.
[62] J. Luo, et al., Arrays of Ni nanowire/multiwalled carbon nanotube/amorphous carbon nanotube heterojunctions containing Schottky contacts, Appl. Phys. Lett. 90 (3) (2007), 033114.
[63] Y. Heo, et al., Pt/ ZnO nanowire Schottky diodes, Appl. Phys. Lett. 85 (15) (2004) 3107–3109.
[64] S.-F. Hu, et al., A silicon nanowire with a Coulomb blockade effect at room temperature, Adv. Mater. 14 (10) (2002) 736–739.
[65] C.S. Lao, et al., ZnO nanobelt/nanowire Schottky diodes formed by dielectrophoresis alignment across Au electrodes, Nano Lett. 6 (2) (2006) 263–266.
[66] Z. Fan, J.G. Lu, Electrical properties of ZnO nanowire field effect transistors characterized with scanning probes, Appl. Phys. Lett. 86 (3) (2005), 032111.
[67] E. Rhoderick, R. Williams, Metal–semiconductor Contacts, second ed., Clarendon., Oxford, 1988.
[68] L.P. Kouwenhoven, D. Austing, S. Tarucha, Few-electron quantum dots, Rep. Prog. Phys. 64 (6) (2001) 701.
[69] J. Appenzeller, et al., Tunneling versus thermionic emission in one-dimensional semiconductors, Phys. Rev. Lett. 92 (4) (2004), 048301.
[70] J.-R. Kim, et al., Electrical transport properties of individual gallium nitride nanowires synthesized by chemical-vapor-deposition, Appl. Phys. Lett. 80 (19) (2002) 3548–3550.
[71] B. Simpkins, P. Pehrsson, A. Laracuente, Electronic conduction in GaN nanowires, Appl. Phys. Lett. 88 (7) (2006), 072111.
[72] M.-H. Ham, D.-K. Oh, J.-M. Myoung, Transport properties in (Ga, Mn) N nanowire field-effect transistors, J. Phys. Chem. C 111 (30) (2007) 11480–11483.